

1 Article

2

Dynamic Measurement Errors Prediction Model of 3 Sensors Based on NAPSO-SVM

4 **Minlan Jiang ^{1,*}, Lan Jiang ¹, Dingde Jiang ^{2,*}, Fei Li ¹ and Houbing Song ³**5 ¹ College of Mathematics, Physics and Information Engineering, Zhejiang Normal University, Jinhua 321004,
6 China;

7 sa1105587@163.com(L.J.); m18329019792@163.com(F.L.)

8 ² School of Astronautics and Aeronautic, University of Electronic Science and Technology of China,
9 Chengdu 611731, China10 ³ Department of Electrical, Computer, Software, and Systems Engineering, Embry-Riddle Aeronautical
11 University, Daytona Beach, FL 32114 USA; h.song@ieee.org

12 * Correspondence: xx99@zjnu.cn(M. Jiang); jiangdd@uestc.edu.cn(D. Jiang); Tel.: +86-138-6797-9259

13

14

15 **Abstract:** Dynamic measurement error correction is an effective method to improve the sensor
16 precision. Dynamic measurement error prediction is an important part of error correction, support
17 vector machine (SVM) is often used to predicting the dynamic measurement error of sensors.
18 Traditionally, the parameters of SVM were always set by manual, which can not ensure the model's
19 performance. In this paper, a method of SVM based on an improved particle swarm optimization
20 (NAPSO) is proposed to predict the dynamic measurement error of sensors. Natural selection and
21 Simulated annealing are added in PSO to raise the ability to avoid local optimum. To verify the
22 performance of NAPSO-SVM, three types of algorithms are selected to optimize the SVM's
23 parameters, they are the particle swarm optimization algorithm (PSO), the improved PSO
24 optimization algorithm (NAPSO), and the glowworm swarm optimization (GSO). The dynamic
25 measurement error data of two sensors are applied as the test data. The root mean squared error
26 and mean absoluter percentage error are employed to evaluate the prediction models'
27 performances. The experiment results show that the NAPSO-SVM has a better prediction precision
28 and a less prediction errors among the three algorithms, and it is an effective method in predicting
29 dynamic measurement errors of sensors.

30

31

32

Keywords: Sensors; Dynamic measurement errors; Prediction; Improved PSO; Support Vector
Machine

33

1. Introduction

34

Today, sensors are widely used in the real world, sensor error is one of the key to evaluate the
35 measurement quality of the sensor results. With the development of modern measurement
36 technology, dynamic measurement has gradually become the mainstream of modern measurement.

37

As an effective theory to improve the measurement accuracy and reduce the measurement error,
38 real-time error correction of sensors have been widely used in the dynamic measurement. Predicting
39 the dynamic measurement error is useful to correct the errors of sensor. Dynamic measurement errors
40 of sensors are difficult to modeling with traditional mathematics cause they has four features[1]: time-
41 varying, randomness, correlation and dynamic. Because its complexity, predicting the dynamic error
42 has been a popular research fields[2-3].

43

In recent years, several modeling methods are used to predict dynamic error like the gray theory,
44 Bayesian networks and neural network. Every method has its own advantages and drawbacks.
45 Harmonic analysis method is suitable to model the periodic sequences, but it is not suitable for the

46 random sequence[4]. Bayesian networks is useful for prediction modeling, however, it requires the
 47 prior distribution and independent samples, which is difficult to achieve in the real systems[5]. Grey
 48 theory model can be constructed by a few samples, but it only depicts a monotonically increasing or
 49 decreasing process[6]. Artificial neural network has a good performance of non-linear mapping,
 50 however, it has disadvantages, such as over-fitting and easy to falls into a local minimum[7].

51 Support vector machine (SVM) adopts structural risk minimization to improve generalization
 52 ability[8]. It can better solve the problems of nonlinear data and small samples. SVM has been widely
 53 applied to solve the problem of function fitting[9]. However, the generalization ability of SVM
 54 depends heavily on the appropriate parameters, the model's parameters has huge influence on the
 55 precision of the model predictions[10-11]. Thus, many optimization algorithms have been adopted to
 56 optimize the SVM parameters, like the particle swarm optimization algorithm, genetic algorithm and
 57 glowworm swarm optimization algorithm. There are limitations in these methods, the particle swarm
 58 optimization and genetic algorithm fall into the local extremes easily[12-14], the glowworm swarm
 59 optimization algorithm has low convergence precision and slow convergence speed[15]. NAPSO
 60 algorithm is an improved particle swarm optimization algorithm based on the natural selection
 61 strategy and simulated annealing mechanism. these two methods are used to improve the global
 62 search ability and convergence speed. In this study, a method of dynamic measurement error
 63 prediction for sensors based on NAPSO optimize support vector machine is proposed.

64 The rest of the paper is organized as follows, in section 2, the overview of SVM algorithm is
 65 provided in detail. Then, in section 3, PSO, NAPSO algorithm and the process of Optimization are
 66 described briefly. Section 4 reports on a simulation of the dynamic measurement error prediction
 67 model. The results of experiments are discussed in section 5. Conclusions are drawn in the last section.

68 2. SVM Algorithm

69 2.1. SVM

70 SVM is a machine learning method based on the statistical learning theory developed in mid-
 71 1990s. The basic idea of SVM is that the data of input space R^n are mapped to a high dimensional
 72 feature space F by a nonlinear mapping, then finish the linear regression operations in the high
 73 dimensional feature space.

74 For a given training dataset $\{(x_i, y_i), i=1,2, \dots, n\}$, x_i is a n-dimensional input vector and y_i
 75 is the corresponding output value, $\phi(x)$ is the nonlinear mapping from input space R^n to high
 76 dimensional feature space F .

$$77 R^n \rightarrow F : x \rightarrow \phi(x) \quad (1)$$

78 The regression function of SVM is formulated as follows:

$$79 f(x) = [\omega \cdot \phi(x)] + b \quad \omega \in R^m, b \in R \quad (2)$$

80 Where ω is the weight vector and b is the threshold, the main goal of the SVM is to find the
 81 optimal ω , the optimization equation can be expressed as follows:

$$82 \begin{aligned} \min_{\omega, \xi} \quad & \phi(\omega) = \frac{1}{2} \|\omega\|^2 \\ \text{s.t.} \quad & |y_i - f(x_i)| \leq \varepsilon, \quad i = 1, 2, \dots, n \end{aligned} \quad (3)$$

83 Where ε is a parameter of the insensitive loss function. In practice, two slack variables ξ_i, ξ_i^* and
 84 a punishment coefficient C are introduced in the equation (3). According to the risk minimization,
 85 equation (3) can be rewritten as the equation (4). The first item of equation (4) is the regularization
 86 part, which is used to smooth the function, improves generalization ability. And the second item is
 87 an empirical error term. C is the punishment coefficient, which can regulate the balance of the two
 88 items.

$$\begin{aligned}
 89 \quad \min_{\omega, \xi} \quad & \varphi(\omega, \xi) = \frac{1}{2} \|\omega\|^2 + C \sum_{i=1}^n (\xi_i + \xi_i^*) \\
 & \text{s.t.} \quad y_i - f(x_i) \leq \xi_i + \varepsilon \\
 & \quad f(x_i) - y_i \leq \xi_i^* + \varepsilon \\
 & \quad \xi_i, \xi_i^* \geq 0 \\
 & \quad (i = 1, 2, \dots, n)
 \end{aligned} \tag{4}$$

90 Introduce the Lagrange multipliers α_i and α_i^* , then the regression problem can be solved by
 91 solving a dual problem as equation(5).

$$\begin{aligned}
 92 \quad \max_{\alpha_i, \alpha_i^*} \quad & W(\alpha_i, \alpha_i^*) = -\frac{1}{2} \sum_{i,j=1}^n (\alpha_i - \alpha_i^*)(\alpha_j - \alpha_j^*) K(x_i, x_j) \\
 & - \varepsilon \sum_{i=1}^n (\alpha_i + \alpha_i^*) + \sum_{i=1}^n y_i (\alpha_i - \alpha_i^*) \\
 & \text{s.t.} \quad \sum_{i=1}^n y_i (\alpha_i - \alpha_i^*) = 0 \\
 & \quad 0 \leq \alpha_i, \alpha_i^* \leq C, \quad i = 1, 2, \dots, n
 \end{aligned} \tag{5}$$

93 Where $K(x_i, x_j)$ is the Kernel function. In the last, the SVM regression function is formulated as:

$$94 \quad f(x) = \sum_{i=1}^n (\alpha_i - \alpha_i^*) K(x_i, x_j) + b \tag{6}$$

95 2.2. Kernel Function

96 Kernel function is a key concept of SVM, the performance of SVM mainly depends on the kernel
 97 function. As shown in the equation (1), the kernel function establishes a relation between the input
 98 space R^n and the high dimensional feature space F . Different selection of kernel functions will
 99 construct different regression models.

$$100 \quad K(x_i, x_j) = \phi(x_i)^T \cdot \phi(x_j) \tag{7}$$

101 The common kernel functions include the polynomial kernel function, linear kernel function,
 102 fourier kernel function and radial basis function (RBF) kernel function. The kernel function
 103 parameters has a directly influence on the complexity of the function, RBF kernel function has the
 104 advantages of fewer parameters and good performance. Thus, RBF kernel function is used in this
 105 paper.

106 The RBF kernel function is expressed as follows:

$$107 \quad K(x_i, x_j) = \exp \left\{ -\frac{|x_i - x_j|^2}{2\sigma^2} \right\} \tag{8}$$

108 Where σ is the width coefficient of the kernel function.

109 The SVM parameters determine both its generalization ability and learning ability, the
 110 punishment coefficient C and RBF kernel function width σ have a directly impact on the accuracy
 111 and efficiency of the SVM prediction model. C adjusts the balance between generalization and
 112 empirical error. When C is greater, the model's complexity will be increased and it will fall into the
 113 "over-fitting" phenomenon easily, if C is too small, the model's complexity will be reduced and it
 114 will fall into the "under-fitting" phenomenon easily. The value of σ affects the complexity of the
 115 sample data distribution in feature space. In this paper, NAPSO algorithm is used to optimize the
 116 two parameters to achieve a better prediction results.

117 3. SVM Parameters Optimization Based On NAPSO

118 3.1. PSO

119 Particle swarm optimization was proposed by Eberhart and Dr. Kennedy in 1995[12], PSO was
 120 derived from research on bird flocks' preying behavior. When a flock of birds is looking for food in
 121 an area randomly, if there is only one piece of food in the area being searched, the most effective and
 122 simple method to find the food is to follow the bird that is closest to the food.

123 In PSO algorithm, every single solution is a particle in the search space. Each particle has a fitness
 124 value, which is determined by an optimization function, each particle has its own velocity and
 125 position. The velocity and position of each particle will be changed by the particle best position and
 126 global best position. The update equations of the velocity and position are shown by the following
 127 expression:

$$v_{i,d}(t+1) = \omega v_{i,d}(t) + c_1 r_1 [p_{best} - x_{i,d}(t)] + c_2 r_2 [g_{best} - x_{i,d}(t)] \quad (9)$$

$$x_{i,d}(t+1) = x_{i,d}(t) + v_{i,d}(t+1) \quad (10)$$

130 In the D-dimensional space, t is the iteration number, $v_{i,d}(t)$ is the velocity of particle i at
 131 iteration t , $v_{i,d}(t+1)$ is the velocity of particle i at iteration $t+1$, $x_{i,d}(t)$ is the position of
 132 particle i at iteration t , $x_{i,d}(t+1)$ is the position of particle i at iteration $t+1$, ω is the
 133 inertia weight. c_1 is the cognition learning factor, c_2 is the social learning factor, r_1 and r_2 are
 134 random numbers that are uniformly distributed in $[0,1]$, p_{best} is the particle best position for the
 135 individual variable of particle i , g_{best} is the global best position variable of the particle swarm.

136 The initial position and velocity of each particle are randomly generated and will be updated
 137 based on the formula (9) and formula (10) until a satisfactory solution is found. In the PSO algorithm,
 138 a single particle moves to its p_{best} and g_{best} , each particle's movement generates fast convergence,
 139 thus PSO algorithm converges rapidly. However, the fast convergence also makes the update of each
 140 particle depend too much on its p_{best} and g_{best} , which makes the algorithm fall into local optimum
 141 and premature convergence easily. Therefore, in this paper, an improved PSO algorithm (NAPSO) is
 142 used to optimize the parameters of SVM.

143 3.2. NAPSO

144 NAPSO algorithm is an improved PSO algorithm based on the methods of natural selection and
 145 simulated annealing. In the NAPSO algorithm, the simulated annealing mechanism is used to
 146 improve the ability of the algorithm to jump out of a local optimum trap, the natural selection method
 147 is employed to accelerate the rate of convergence.

148 NAPSO algorithm starts with a set of random velocities and positions. Before the iteration, each
 149 particle's personal best position and global best position are calculated by the fitness function. Each
 150 particles update its velocity and position by the formula (9) and formula (10) at each iteration.

151 After updating a particle's speed, position l and fitness value f' , the particle moves to a
 152 random position l'_1 in its neighborhood and computes its new fitness value f'_1 . The movement
 153 formula is expressed as follows:

$$l'_1 = l + r_3 * [v_{max} - v_{min}] * r_4 \quad (11)$$

154 Where r_3 is the normally distribution random numbers of D-dimension that are distributed in $[0,1]$,
 155 r_4 is a random number that is uniformly distributed in $[0,1]$, v_{max} is the maximum value of the
 156 velocity, and v_{min} is the minimum value of the velocity.

157 When $f'_1 > g_{best}$, keep the position l . When $f'_1 < g_{best}$, if $f'_1 < f'$, use the new position l'_1
 158 to replace the position l ; if $f'_1 > f'$, use the new position l'_1 to replace the position l by the
 159 simulated annealing operation, the operation of simulated annealing is expressed as follows:

161

$$l = \begin{cases} l & \text{if } \exp((-1)*(f'_l - f')/T) > r4 \\ l'_l & \text{if } \exp((-1)*(f'_l - f')/T) \leq r4 \end{cases} \quad (12)$$

162 Where r_4 is a random number that is uniformly distributed in $[0,1]$, T is the simulated annealing
163 temperature.

164 Each particle uses the simulated annealing operation to determine whether to accept the new
165 position, and then updates the particle's p_{best} and g_{best} by its position. The simulated annealing
166 operation can significantly enhance the ability of the algorithm to jump out of the local optimum trap.
167 At the end of each iteration, all particles have been ranked by their fitness values, from best to worst,
168 and using the better half to replace the other half. In this way, the stronger adaptability particles are
169 saved. Finally, the NAPSO algorithm is terminated by the satisfaction of a termination criterion.

170 The pseudo code of the NAPSO algorithm is presented as follows:

Algorithm NAPSO

Input ω, c_1, c_2, T

Output g_{best}

Initialization: x, p_{best}, g_{best}

while $t < \text{maximum number of iterations}$ and $g_{best} > \text{minimum fitness}$ **do**

for each particle **do**

 update the velocity v , position l , and fitness f'

 find a new position l'_l in the neighborhood and Calculate its fitness value f'_l

if1 ($f'_l < g_{best}$) **then**

if2 ($f'_l - f' < 0$) **then**

 accept the new position l'_l

else if2

 accept the new position l'_l by the simulated annealing operation

end if2

else if1

 accept the old position l

end if1

 update the p_{best}, g_{best} and Simulated temperature T

end for

 rank all particles by their fitness value, use the better half to replace the other half.

$t=t+1$

end while

 return the g_{best}

171 The simulated annealing operation will slow the rate of convergence, thus increasing the
172 convergence time. The natural selection operation will reduce the sample diversity of samples.
173 However, these two operations can compensate for each other, the simulated annealing operation
174 can increase sample diversity, and the natural selection operation can speed up the convergence rate.
175 These two operations are used to both ensure the convergence rate of the algorithm and guarantee
176 that the ability of the algorithm to jump out of the local optimal trap can be enhanced.

177 *3.3. Optimization Process*

178 The NAPSO algorithm is applied to optimize the SVM parameters C and σ as follows:

179 Step 1: Initialize the NAPSO algorithm, set the number of particles velocity, particles positions
180 and the other parameters. Because the search space is 2 dimensional, the position of each particle
181 contains two variables. Set T to be the simulated temperature; the initial T is 5000°C , and the

182 lower limit of T is 1°C. Calculate the fitness value of each particle. The fitness evaluation function
 183 is defined as follows:

184

$$J = \sum_{i=1}^n (Y_i - Y'_i)^2 / n \quad (13)$$

185 Where Y_i is the actual value, Y'_i is the predicted value and n is the number of the training samples.

186 Step 2: According to the fitness value of each particle to set the personal best position p_{best} and
 187 global best position g_{best} .

188 Step 3: Update the position l and velocity of each particle. Evaluate the fitness value f' . Then,
 189 randomly find a new position l'_1 in the neighborhood of the particle, calculate the new fitness value
 190 (f'_1) of the new position.

191 Step 4: Calculate the difference between the fitness value f' and the new fitness value f'_1 ,
 192 $\Delta f = f'_1 - f'$.

193 Step 5: When $f'_1 \geq g_{best}$, keep the original position l . When $\Delta f > 0$ and $f'_1 < g_{best}$,
 194 according the formula (12) to accept the new position l'_1 , if $\Delta f < 0$ and $f'_1 < g_{best}$, replace the
 195 original position with the new position. Then, update the p_{best} and g_{best} .

196 Step 6: When the updates of each particle has completed, then rank all of the particles according
 197 to the each particle's fitness value, employ the better half particles' information to replace the other
 198 half particles' information and update the temperature $T = T * 0.9$.

199 Step 7: If the termination conditions are satisfied, output the two variables of the g_{best} ;
 200 Otherwise, return to Step 2.

201 4. Experiments

202 4.1. Data Description

203 In this paper, two cases have been considered to illustrate the effectiveness of the proposed
 204 method. The data of case 1 is the dynamic error sequence, which is derived from the measuring error
 205 of the angular instrument with anticlockwise rotation (speed 2r/min) based on standard value
 206 interpolation under room temperature, the error sequence contains a total of 240 samples. In case 2,
 207 the measuring error sequence of the length grating contains a total 141 samples. The process of
 208 collecting data is expressed as follows: the measurement range is 500mm and the sample interval is
 209 25mm, the computer receive the actual displacement from the laser interferometer and the measuring
 210 displacement from the length grating. The difference of the two data is the dynamic measurement
 211 error of the length grating.

212 4.2. Preprocessing

213 The two datasets both are one-dimensional data, in order to achieve the better predict results
 214 and get more information from the data, these two one-dimensional data must be converted to multi-
 215 dimensional data[16]. Assuming p is the dimension of the input vector, the reconstructed samples
 216 are listed in Table 1.

217 According to the reconstructed method listed in the Table 1, in case 1, the dimension number p
 218 is 16, the number of restructured sample is 224, selecting the first 124 samples for training and the
 219 final 100 samples for testing. The proportion of training samples to testing samples is 1.24:1, in case
 220 2, the dimension p is 12, the number of restructured sample is 129, the first 100 samples are selected
 221 as training data and the rest are used as testing data. The proportion of training samples to testing
 222 samples is 3.44:1.

223

Table 1. Reconstructed samples.

| Input | Output |
|-----------------------------------|----------|
| $X(1), X(2), \dots, X(p)$ | $X(p+1)$ |
| $X(2), X(3), \dots, X(p+1)$ | $X(p+2)$ |
| ... | ... |
| $X(n-p), X(n-p+1), \dots, X(n-1)$ | $X(n)$ |

224 Preprocess the data by the normalized method, then perform parameter optimization and train
 225 the model.

226 *4.3. Valuation Index*

227 To further evaluate the prediction of the NAPSO-SVM model, the root mean square error
 228 (RMSE) and mean absolute percent error(MAPE) are used as evaluation indices. The definition of
 229 MAPE and RMSE are expressed as follows:

$$230 \quad \text{RMSE} = \sqrt{\frac{1}{n} \sum_{i=1}^n (Y_i - Y'_i)^2} \quad (14)$$

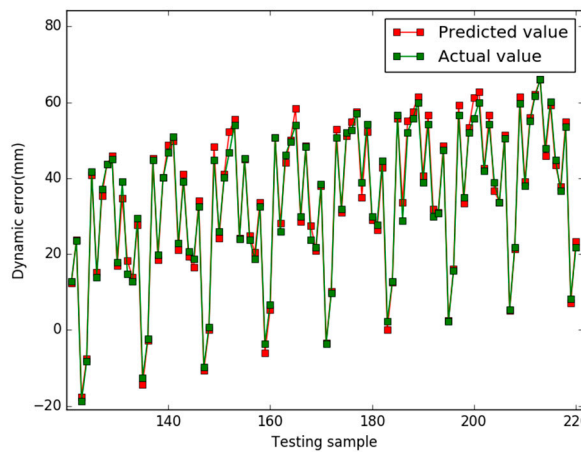
$$231 \quad \text{MAPE} = \frac{1}{n} \sum_{i=1}^n \left| \frac{Y_i - Y'_i}{Y_i} \right| \quad (15)$$

232 Where Y_i is the actual value, Y'_i is the prediction value and n is the number of the training
 233 sample.

234 Using the NAPSO algorithm to determine the punishment coefficient C and RBF kernel
 235 function width σ . The SVM model is built based on the training samples and optimal parameters.
 236 To show the performance of the proposed method, the particles swarm optimization and glowworm
 237 swarm optimization are also implemented.

238 **5. Results**

239 In case 1, the prediction results of three models are shown in Figures. 1, 2 and 3, respectively.



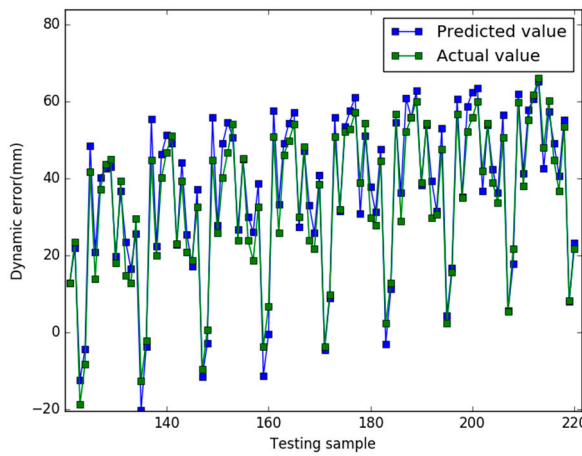
240

Figure 1. Predicted results of the NAPSO-SVM (case1)

241 To make a fair comparison, the maximum generation, population size, minimum fitness value,
 242 range of gains, dimension of search space and initial positions are identical for all the algorithms. The
 243 maximum number of generations is 100, the minimum fitness value is 0.1, the size of the population
 244 is 100, and the dimension of the search space is 2. The parameters for NAPSO were set as follows: the
 245 inertia weight $w = 0.9$, the acceleration constant c_1 and c_2 are 2, the initial temperature is
 246 10000°C , the lower limit of temperature is 1°C , the maximum value of velocity is 1, the minimum
 247 value of velocity is -1. In GSO algorithm, the light absorption coefficient is 50, the minimum value of
 248

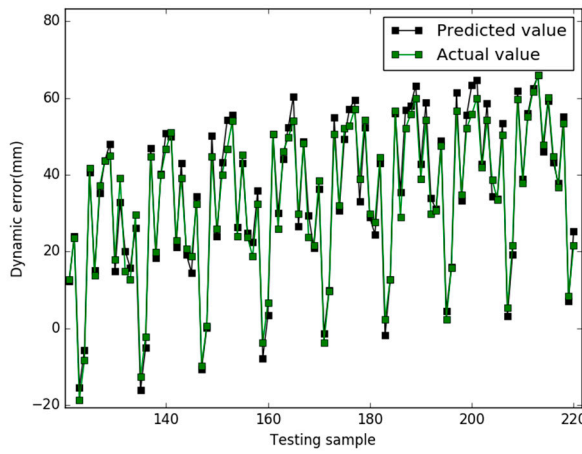
249 attractiveness is 0.8, the maximum value of attractiveness is 1.0, the value of initial step size factor is
 250 0.5. The PSO algorithm has the same inertia weight and acceleration constant as the NAPSO
 251 algorithm.

252 Figure.4 presents the comparison results of predicted residuals by the three models. The MAPE
 253 value and RMSE value of the three models are listed in Table 2.



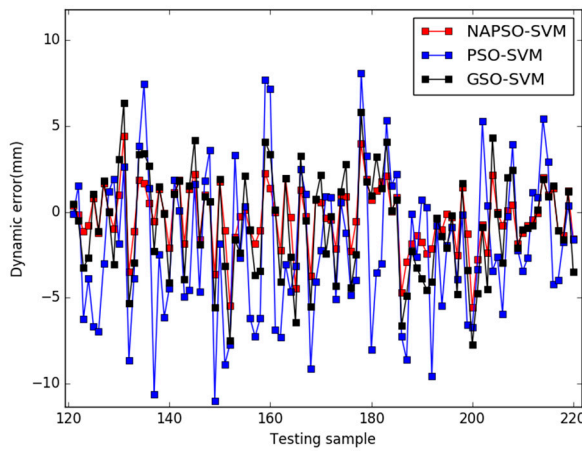
254
255

Figure 2. Predicted results of the PSO-SVM (case1)



256
257

Figure 3. Predicted results of the GSO-SVM (case1)



258
259

Figure 4. Comparison of three models for predicted residuals (case 1)

260 By comparing Figures. 1-3, we find that the NAPSO-SVM model outperforms the PSO-SVM and
 261 GSO-SVM model. The prediction performance of NAPSO-SVM is better than GSO-SVM model and
 262 accuracy much better than PSO-SVM.

263 The residual curves of the three models are shown in the Figure. 4, The prediction residual curve
 264 of the PSO-SVM model is large, ranging from -11 to 8", and the prediction residual of the GSO-SVM
 265 model is smaller than the PSO-SVM model. But it is still relatively large, ranging from -8 to 6". The
 266 predicted residual of the NAPSO-SVM is smaller than the others and tends to more gentle, ranging
 267 from -5 to 4". The results prove that dynamic measurement error prediction ability of NAPSO-SVM
 268 model is better than PSO-SVM and GSO-SVM model, and the NAPSO algorithm is an effective
 269 method for parameters optimization.

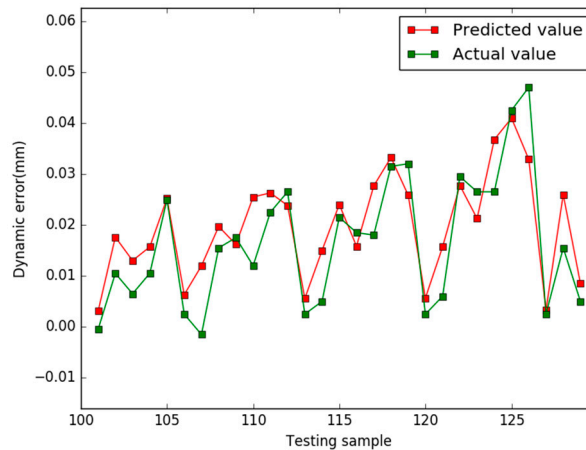
270 To further verify the ability of the three models. Table 2 lists the comparison results between the
 271 three models for prediction accuracy indexes.

272 **Table 2.** Comparison of the index value among the three models (case 1).

| MODEL | MAPE | RMSE |
|-----------|--------|--------|
| NAPSO-SVM | 0.0744 | 0.1879 |
| PSO-SVM | 0.2423 | 0.4710 |
| GSO-SVM | 0.1493 | 0.3128 |

273 In Table 2, the MAPE value and RMSE value of the NAPSO-SVM model are smaller than the
 274 PSO-SVM and GSO-SVM model. The MAPE value is approximately 0.0744 for NAPSO-SVM model
 275 compared with approximately 0.2423 and 0.1493 for the PSO-SVM and GSO-SVM model, respectively.
 276 Furthermore, the RMSE value is 0.1876 in the case of NAPSO-SVM model. Compared with the
 277 NAPSO-SVM model, the RMSE value of the GSO-SVM model and PSO-SVM model are 0.4710 and
 278 0.3128 respectively. In summary, the results of the Table 2 are accorded with the Figure. 4, the
 279 NAPSO-SVM model has the best dynamic measurement error prediction ability among the three
 280 methods.

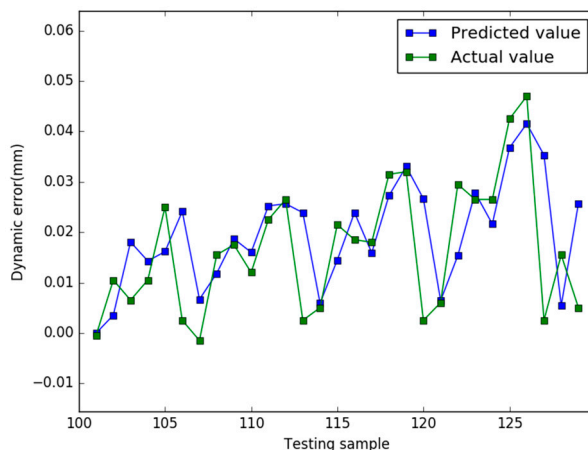
281 In case 2, the parameters of each algorithm are essentially the same as the previous case, the
 282 prediction results of three models are shown in Figures.5, 6 and 7. Figure.8 shows the comparison
 283 results of predicted residuals by three models. The MAPE value and RMSE value of the three models
 284 are listed in the Table 3.



285

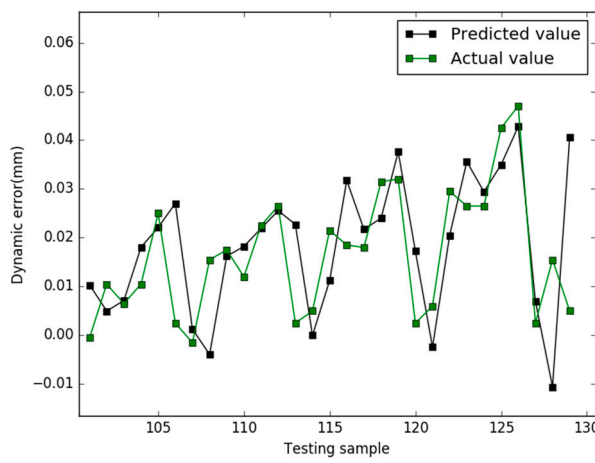
286 **Figure 5.** Predicted results of the NAPSO-SVM (case 2)

287 In Figures.5-7, when the ratio of training samples and testing samples is approximately 3.5, the
 288 prediction curve of the NAPSO-SVM model is closest to the actual value curve, and the prediction
 289 curve of the NAPSO-SVM model is approximately the same as the actual value curve. However,
 290 unlike the case 1, The prediction results of the PSO-SVM model is better than the PSO-SVM model,
 291 but the prediction curves of these two models still lag behind the actual value curve.



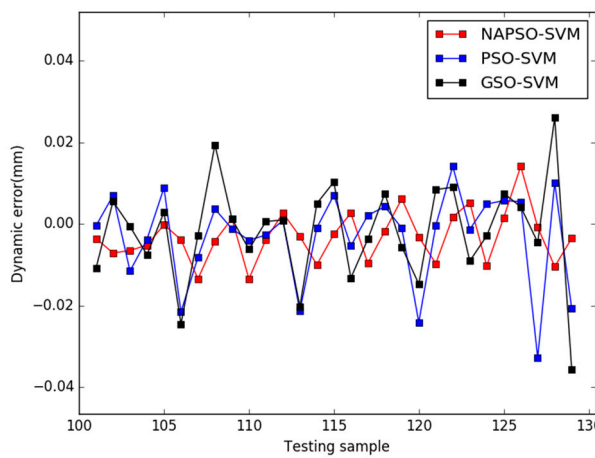
292

293

Figure 6. Predicted results of the PSO-SVM (case 2)

294

295

Figure 7. Predicted results of the GSO-SVM (case2)

296

297

Figure 8. Comparison of the predicted residuals of the three models(case2)

298

299

300

301

In Figure.8, the prediction residual of the NAPSO-SVM model is smallest among the three models, ranging from -0.013 to 0.014 mm. The prediction residual of the GSO-SVM model is ranging from -0.035 to 0.026 mm, and the prediction residual of the PSO-SVM model is ranging from -0.032 to 0.013 mm.

302

Table 3. Comparison of the index value among the three models (case 2).

| MODEL | MAPE | RMSE |
|-----------|--------|--------|
| NAPSO-SVM | 1.0833 | 0.0013 |
| PSO-SVM | 1.9714 | 0.0021 |
| GSO-SVM | 2.2948 | 0.0023 |

303 As Table 3 shows, the MAPE value is approximately 1.0833 for the NAPSO-SVM model
 304 compared with approximately 1.9714 and 2.2948 for the PSO-SVM model and GSO-SVM model.
 305 NAPSO-SVM model has the smallest RMSE value of the three algorithms, acquiring RMSE value of
 306 0.0013 and the RMSE values of the PSO-SVM model and GSO-SVM model are 0.0021 and 0.0023,
 307 respectively. The prediction ability of the NAPSO-SVM model is clearly better than the other models,
 308 and GSO-SVM model has the worst performance.

309 The results of the two cases show that the NAPSO-SVM model has the best prediction accuracy
 310 among the three methods. This indicate that the NAPSO algorithm has the better capability of global
 311 search than the other two algorithm, the reason is that the updating of the position and velocity of
 312 the particles in the PSO algorithm are dependent too much on current best particle. Compared with
 313 the PSO algorithm, the NAPSO algorithm uses the simulated annealing and natural selection
 314 mechanism, it is easier jump out of the local trap and search the global optimal solution in the global
 315 space.

316 6. Conclusions

317 Dynamic measurement has been a hot area of research for several years, and dynamic
 318 measurement error prediction is an useful method to improve the sensor measurement accuracy. In
 319 this study, a method of dynamic measurement error prediction based on NAPSO-optimized SVM
 320 parameters is proposed. To improve the prediction accuracy, the NAPSO algorithm is used to
 321 optimize the SVM parameters to avoid the problems of “over-fitting” and “under-fitting” of SVM.
 322 The results of the two cases show that compared with the PSO-SVM and GSO-SVM model, the
 323 NAPSO-SVM model has the better prediction accuracy. The proposed method provides a new way
 324 for predicting the sensor’s dynamic measurement error and has definite value for application in
 325 dynamic measurement. However, like the standard PSO, NAPSO has the intrinsic property
 326 randomness. In the future, we plan to study which is the more effective method for improving the
 327 prediction results.

328 **Acknowledgments:** The work was supported in part by the National Natural Science Foundation of China (Nos.
 329 51305407, 61571104).

330 **Author Contributions:** M.J. and L.J. were the main designers of the proposed scheme and wrote the paper. F.L.
 331 focused on the research, and part of the paper writing, D.J. and H.S. revised the paper and analyzed the results.

332 **Conflicts of Interest:** The authors declare no conflict of interest.

333 References

1. Yakovlev, V.T. Method of Determining dynamic Measurement Error Due to Oscillographs. *Measurement Techniques* **1987**, *30*, 331-334.
2. Chen, Y. Area-Efficient Fixed-Width Squarer with Dynamic Error-Compensation Circuit. *IEEE Transactions on Circuits and Systems II: Express Briefs* **2015**, *62*, 851-855.
3. Yakovlev, V.T.; Collins, E.; Flores, K.; Pershad, P.; Stemkovski, M.; Stephenson, L. Statistical Error Model Comparison for Logistic Growth of Green Algae (*Raphidocelis subcapitata*). *Applied Mathematics Letters* **2017**, *64*, 213-222.
4. Trapero, J.; Kourentzes, N.; Martin, A. Short-term solar irradiation forecasting based on dynamic harmonic regression. *Energy* **2015**, *84*, 289-295.
5. Yang, H.; Zhang, L.; Zhou, J.; Fei, Y.; Peng, D. Modelling of dynamic measurement error for parasitic time grating sensor based on Bayesian principle. *Guangxue Jingmi Gongcheng/Optics and Precision Engineering* **2015**, *24*, 2523-2531.

346 6. Ge, L.; Zhao W.; Zhao, S.; Zhou, J. Novel error prediction method of dynamic measurement lacking
347 information. *Journal of Testing and Evaluation* **2012**, *40*, n1.

348 7. Barbounis, T.G.; Theocharis, J.B. A locally recurrent fuzzy neural network with application to the wind
349 speed prediction using spatial correlation. *Neurocomputing* **2007**, *70*, 1525-1542.

350 8. Sasikala, S.; Balamurugan, S.; Geetha, S. A Novel Memetic Algorithm for Discovering Knowledge in Binary
351 and Multi Class Predictions Based on Support Vector. *Machine Applied Soft Computing Journal* **2016**, *49*, 407-
352 422.

353 9. Malvoni M.; De G.; M, G.; Photovoltaic Forecast Based on Hybrid PCA-LSSVM Using Dimensionality
354 Reduced Data. *Neurocomputing* **2016**, *211*, 72-83.

355 10. Wang X.; Kang M.; Fu X.; Li C. Predictive Modeling of Surface Roughness in Lenses Precision Turning
356 Using Regression and Support Vector Machines. *International Journal of Advanced Manufacturing Technology*
357 **2016**, *87*, 1273-1281.

358 11. Suganyadevi, M.; Babulal, C. Support Vector Regression Model for the Prediction of Loadability Margin of
359 a Power System. *Applied Soft Computing* **2014**, *24*, 304-315.

360 12. Kennedy J.; Eberhart R. Particle Swarm Optimization. In Proceedings of the First IEEE International
361 Conference on Neural Networks, Perth, Australia, 1995; pp, 1942-1948.

362 13. Liu Y. Study on an Improved PSO Algorithm and its Application for Solving Function Problem.
363 *International Journal of Smart Home* **2016**, *10*, 51-62.

364 14. Zhong Y.; Ning J.; Zhang H. Multi-agent Simulated Annealing Algorithm based on Particle Swarm
365 Optimisation Algorithm. *International Journal of Computer Applications in Technology* **2012**, *43*, 335-342.

366 15. Zainal N.; Zain A.; Radzi N.; Glowworm Swarm Optimization (GSO) for optimization of machining
367 parameters. *Journal of Intelligent Manufacturing* **2016**, *27*, 998-1006.

368 16. Jiang M.; Luo J.; Jiang D.; Xiong J.; Song H.; Shen J. A Cuckoo Search-support Vector Machine Model for
369 Predicting Dynamic Measurement Errors of Sensors. *IEEE Access* **2016**, *PP*, 99.

370